

# Ground Movements due to Shallow Tunnels in Soft Ground. II: Analytical Interpretation and Prediction

Federico Pinto<sup>1</sup>; Despina M. Zymnis, S.M.ASCE<sup>2</sup> and Andrew J. Whittle, M.ASCE<sup>3</sup>

**Abstract:** This paper considers the practical application of analytical solutions for estimating ground movements caused by shallow tunneling in soft ground using closed-form expressions presented in a companion paper based on linearly elastic and average-dilation models of soil behavior. The analytical solutions express two-dimensional distributions of ground deformations as functions of three parameters: the uniform convergence and relative ovalization of a circular tunnel cavity, and either the Poisson's ratio or the average dilation angle for elastic and plastic behavior, respectively. This paper shows that the analytical predictions can achieve very good representations of the distribution of far field deformations through a series of case studies in clays and sands. In some cases, the input parameters can be interpreted from a simple calibration to three independent measurements of ground displacements comprising surface settlements above the tunnel centerline and at a reference offset, and the lateral displacement at the spring line elevation, recorded by an inclinometer at an offset of one tunnel diameter from the centerline. However, it is generally more reliable to use a least-squares fitting method to obtain the model input parameters, using all available extensometer and inclinometer data. DOI: 10.1061/(ASCE)GT.1943-5606.0000947. © 2013 American Society of Civil Engineers.

**Author keywords:** Tunnels; Deformation; Analytical techniques; Measurement; Elasticity; Plasticity.

## Introduction

All methods of tunneling have the potential to produce deformations in the surrounding soil. Figs. 1(a and b) illustrate the primary sources of movement for cases of closed-face shield tunneling and open-face sequential support and excavation (i.e., conventional tunneling), respectively. For closed-face shield tunneling [e.g., earth pressure balance (EPB) or slurry support], ground movements resulting from stress changes around the tunnel face may be less significant than those caused by overcutting or plowing of the shield or ground loss around the tail void. In contrast, the large changes in stresses around the tunnel heading are clearly important factors for tunnels built by conventional tunneling, and are typically mitigated by local reinforcement, pre-support or improvement, or by reducing the round length. In either case, the three-dimensional (3D) nature and complexity of the sources of ground movement are readily apparent (even without accounting for stratigraphic variations, groundwater conditions, etc.).

Current geotechnical practice relies almost exclusively on empirical methods for estimating tunnel-induced ground deformations. Following Peck (1969) and Schmidt (1969), there is extensive experience in characterizing the transverse surface settlement trough using a Gaussian function

$$u_y(x, y) = u_y^0 \exp\left(\frac{-x^2}{2x_i^2}\right) \quad (1)$$

where  $x$  = horizontal distance from the tunnel centerline;  $y$  = depth below the ground surface;  $u_y^0$  = surface settlement above the tunnel centerline; and the location of the inflection point,  $x_i$ , defines the trough shape.

Mair and Taylor (1997), show that the width of the surface settlement trough can be well correlated to the tunnel depth,  $H$ , and to characteristics of the overlying soil [see Fig. 2(a)]. The trough width ratio varies from  $x_i/H = 0.35$  for sand to 0.50 for clays. They also attempted to extend the same framework to subsurface vertical movements by characterizing the trough width parameter as a function of depth

$$x_i = K(H - y) \quad (2)$$

This involves significantly more uncertainty and requires an empirical function to define  $K$  as shown in Fig. 2(b). There is also very limited data for estimating the horizontal components of the ground movements. The most commonly used interpretation is to assume that the displacement vectors are directed to the center of the tunnel as proposed by Attewell (1978) and O'Reilly and New (1982) such that

$$u_x = \left(\frac{x}{H}\right)u_y \quad (3)$$

The companion paper (Pinto and Whittle 2013) presented and compared a series of analytical solutions for estimating ground movements around shallow tunnels. These kinematic solutions make gross approximations of real soil behavior (either linear elastic or plastic with constant dilation) and disregard the gravitational gradient of in situ stress, yet otherwise fulfill the principles of continuum mechanics. The effectiveness of these analytical solutions resides in the fact that the complete field of ground movements ( $u_x, u_y$  for the transverse plane) can be described by means of three parameters, two of which characterize the modes of tunnel deformation around the tunnel cavity:  $u_\epsilon$ , the uniform convergence, and  $\rho (= -u_\delta/u_\epsilon)$ , the relative distortion; and one soil property, either Poisson's ratio,  $\nu$ , for the elastic case or  $\alpha$ , the average dilation for plastic soil deformation [see Fig. 3].

<sup>1</sup>Associate Professor, FCEfYN Universidad Nacional de Córdoba - CONICET, Córdoba 5016, Argentina.

<sup>2</sup>Ph.D. Candidate, Massachusetts Institute of Technology, Cambridge, MA 02139.

<sup>3</sup>Professor, Massachusetts Institute of Technology, Cambridge, MA 02139 (corresponding author). E-mail: ajwhittl@mit.edu

Note. This manuscript was submitted on August 16, 2011; approved on April 9, 2013; published online on April 13, 2013. Discussion period open until May 3, 2014; separate discussions must be submitted for individual papers. This paper is part of the *Journal of Geotechnical and Geoenvironmental Engineering*, © ASCE, ISSN 1090-0241/04013041(11)/\$25.00.

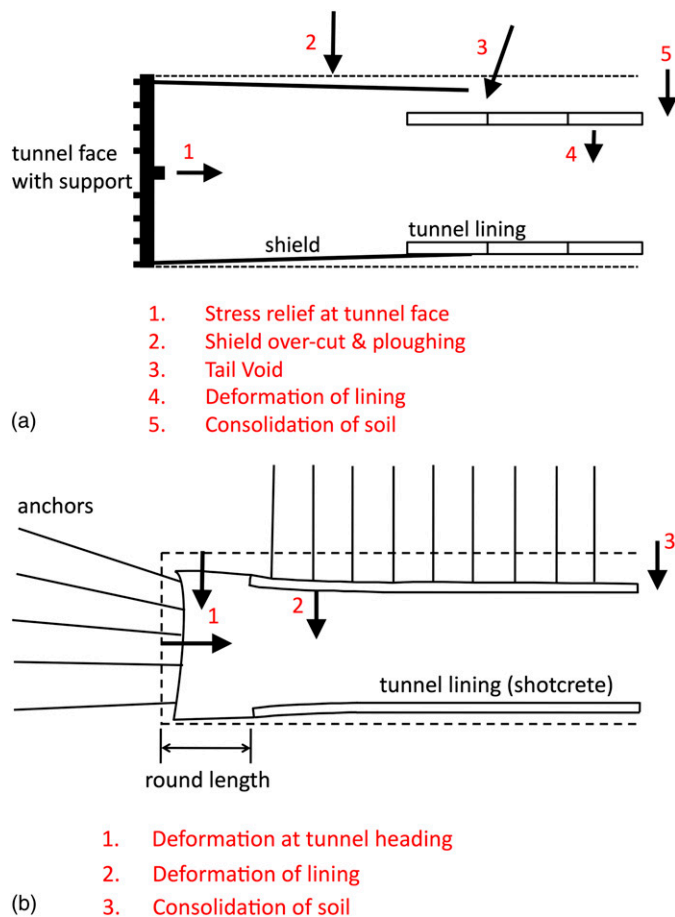


**Fig. 1.** Sources of ground movements associated with tunneling: (a) closed-face tunnel (Mair and Taylor 1997; © 1997 Taylor & Francis Group, London, U.K. Used with permission); (b) sequential excavation (Möller 2006; with permission from Sven Möller)

This paper presents a detailed evaluation of the approximate, closed-form analytical solutions obtained by superposition of singularity solutions (Pinto and Whittle 2013) through a series of case studies. Although similar validation studies have been reported elsewhere (e.g., González and Sagaseta 2001) this work demonstrates the capabilities of the analyses for representing the distribution of ground movements induced by different tunneling methods in a variety of ground conditions. The reliability of these predictions is of critical importance in estimating the effects of tunnel-induced ground deformations on adjacent facilities such as pipelines (Vorster et al. 2005) or pile foundations (Kitiyodom et al. 2005). The goal of the paper is to establish the analytical solutions as a credible alternative to existing empirical methods as well as a useful tool for checking more elaborate numerical analyses. The current validations use published data from six projects to define typical ranges of the input parameters for a range of ground conditions and tunneling methods. Further case studies are clearly needed to compile a more comprehensive database in order for the analyses to be used in estimating the performance of different tunneling methods.

## Evaluation of Input Parameters

In principle, the input parameters for the analytical solutions can be derived from three independent field measurements. Surface settlements are routinely measured in tunnel projects. However, there is no

standardization in the layout of instrumentation for monitoring subsurface movements. Pinto (1999) proposed a procedure that uses the following field measurements with sign convention shown in Fig. 3:

1. The vertical surface displacement above the centerline of the tunnel,  $u_y^0$ ;
2. The vertical surface displacement at a reference offset,  $x/H = 1$ , where  $H$  is the depth to the tunnel spring line,  $u_y^1$ ; and
3. The horizontal displacement at the elevation of the tunnel spring line ( $y/H = -1$ ) measured by a reference inclinometer installed at an offset of one radius from the tunnel wall (i.e.,  $x/R = 2$ ),  $u_x^0$ .

The surface settlement ratio,  $u_y^1/u_y^0$ , is a measure of the trough shape and is highly sensitive to variations in the relative distortion,  $\rho$ , and dilation parameter,  $\alpha$ , as shown in Fig. 4(a). Similarly, the horizontal displacements in the reference inclinometer (i.e., the measurement ratio,  $u_x^0/u_y^0$ ) are also controlled by  $\nu$ ,  $\rho$ , and  $\alpha$ , as illustrated in Fig. 4(b).

Fig. 5(a) shows that it is possible to define unique values of  $\rho$ ,  $\nu$ , or  $\alpha$  from these two measurement ratios. It is important to note that the linearly elastic and average dilation solutions coincide for the case where  $\nu = 0.5$  and  $\alpha = 1$ , corresponding to undrained shearing associated with short-term ground movements of tunnels constructed in low permeability clays. Finally, the uniform convergence of the tunnel cavity,  $u_\varepsilon$ , can be obtained by matching the analytical and measured centerline surface displacements,  $u_y^0$ , as shown in Fig. 5(b), from which the ground loss at the tunnel cavity can be obtained directly,  $\Delta V_L/V_0 = -2u_\varepsilon/R$ .

An alternative approach to parameter selection is to use a least-squares fitting approach to the available vertical and horizontal displacements. Surveys of surface settlements typically involve up to 5–10 offset locations (at a given section), while subsurface movements are usually obtained from measurements in a small number of vertical boreholes. Vertical movements are measured using rod or multipoint borehole extensometers, and horizontal displacements (in two orthogonal directions) are obtained from tilt measurements using inclinometers. The current least-squares fitting method considers each displacement component independently and uses a balanced number of vertical and horizontal measurements, excluding points that are very close to the tunnel, where far-field and constitutive approximations in the analytical solutions become significant (Pinto and Whittle 2013).

The current applications focus on least-squares solutions for the tunnel cavity deformation parameters (i.e.,  $u_\varepsilon$ ,  $u_\delta$ , or  $\rho$ ) based on assumed values of the soil properties ( $\nu$  or  $\alpha$ ). The square solution error (SS) is defined as

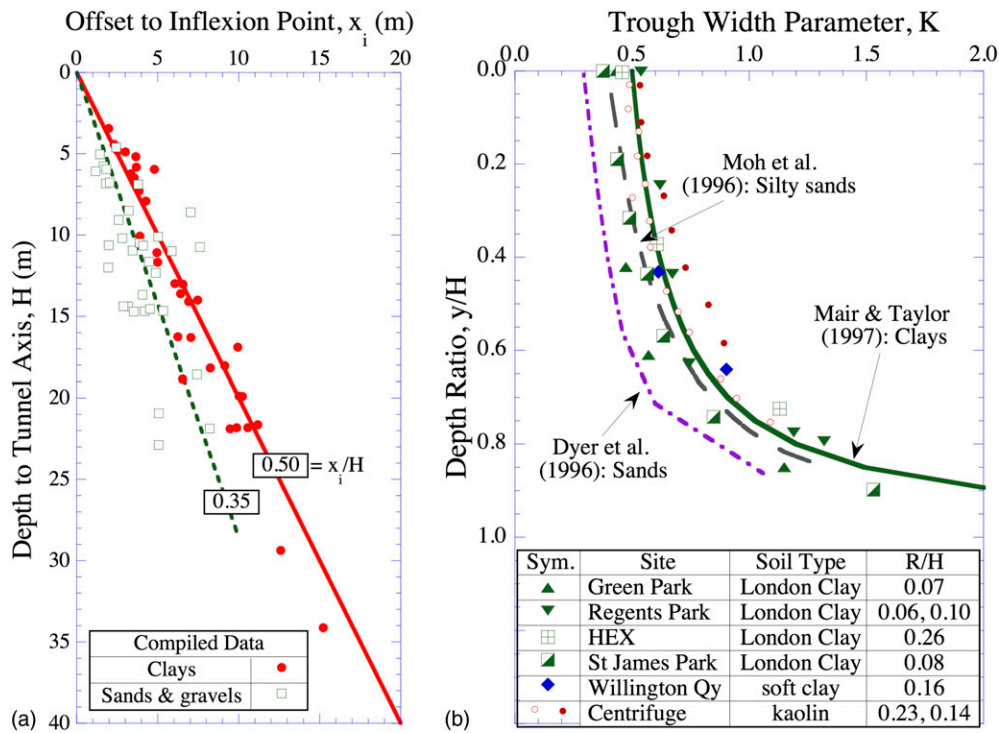
$$SS = \sum_i \left[ (\tilde{u}_{xi} - u_{xi})^2 + (\tilde{u}_{yi} - u_{yi})^2 \right] \quad (4)$$

where  $(\tilde{u}_{xi}, \tilde{u}_{yi})$  = measured displacement components at location  $i$ ; and  $(u_{xi}, u_{yi})$  = computed values at the same location for given set of the input parameters  $(u_\varepsilon, u_\delta)$ .

The input parameters can then be optimized from the global minimum error [least-squares solution (LSS)], as shown in Fig. 6. In most practical cases, engineers will expect to fit the measured centerline surface settlement,  $\tilde{u}_y^0$ , hence, the preferred approach is to present a modified least-squares solution, LSS\*, that includes this additional constraint.

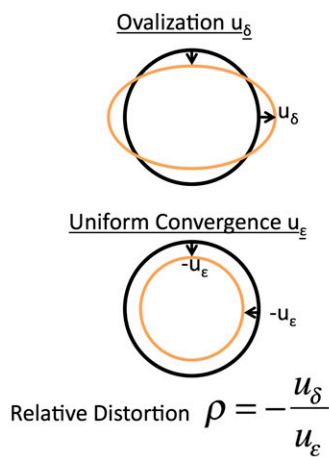
## Case Studies

Table 1 lists the projects considered in this paper and summarizes the model input parameters used in the analyses. The case studies selected



**Fig. 2.** Empirical estimation of inflection point: (a) width of surface settlement troughs; (b) width of subsurface settlement troughs (Mair and Taylor 1997; © 1997 Taylor & Francis Group, London, U.K. Used with permission)

**Model Input Parameters:**



**3-point matching technique:**

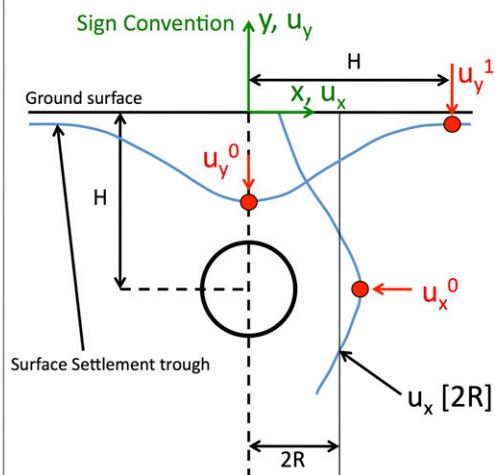


**Fig. 3.** Sign convention and reference parameters for three-point matching method

represent some of the very few tunneling projects where both vertical and horizontal ground measurements were reported, to demonstrate the capability of the analytical solutions to successfully describe horizontal displacements as well as vertical.

**EPB Tunnel in Recent Bay Mud (N-2 Contract), San Francisco**

The San Francisco Clean Water Project N-2 contract was the first U.S. project to use an EPB shield (3.7-m outer diameter) to construct

a 3.56-m-diameter tunnel through recent San Francisco Bay mud (Clough et al. 1983; Finno and Clough 1985). The project included four lines of instrumentation to measure subsurface ground displacements, each with five inclinometers equipped with telescoping couplings to enable vertical displacements to be measured at 3-m intervals.

Fig. 7(b) shows the typical profile at the site (near instrumentation Line Number 4,  $R/H = 0.19$ ) comprising 6.6 m of rubble fill underlain by 7.1 m of Recent Bay Mud, colluvium, and residual sandy clay. Clough et al. (1983) report undrained shear strengths of the

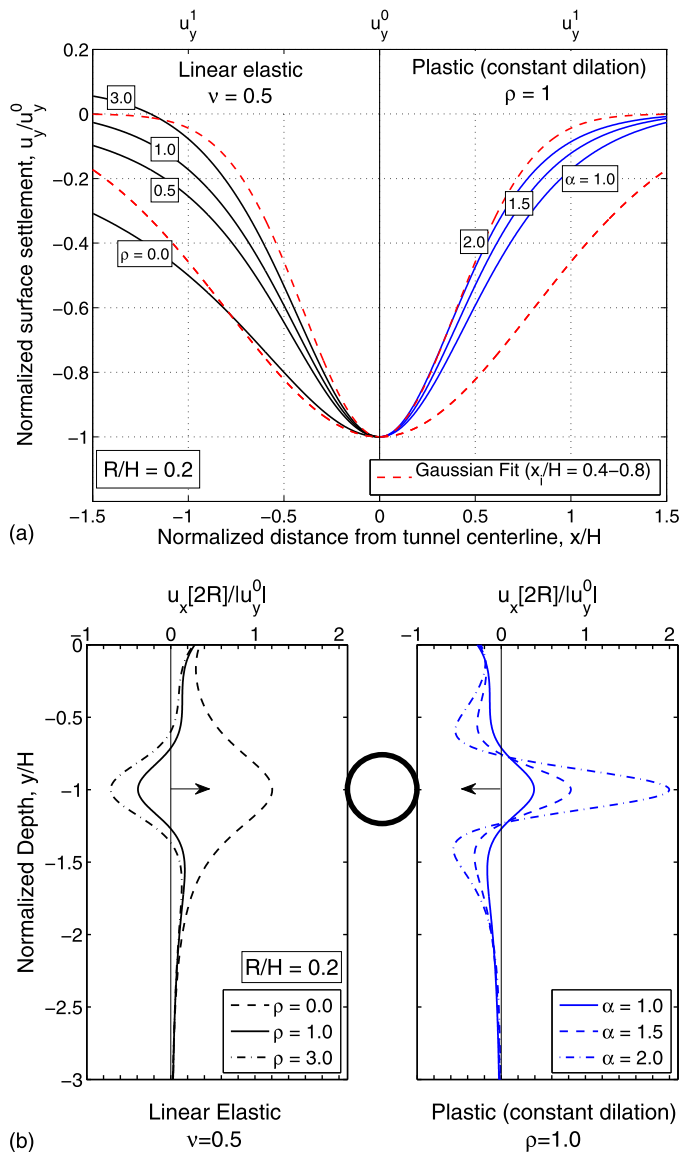


**Fig. 4.** Typical analytical predictions of surface settlements and subsurface lateral displacements: (a) effect of input parameters  $r$  and  $\alpha$  on shape of surface settlement trough; (b) effect of parameters  $r$  and  $\alpha$  on lateral displacements at offset,  $x/2R = 1$

Recent Bay Mud (from UU triaxial tests) increasing with depth from  $s_u = 24 - 28$  kPa, and overload factors ( $\gamma H/s_u$ ) in the range of 5–6. Hence, large zones of plasticity can be expected within the soft clay. The authors also reported that the actual tunnel construction used relatively high face pressure near Line Number 4, ( $p/\gamma H = 0.8$ ) resulting from clogging in the screw auger. Fig. 7(a) shows the surface and subsurface settlements measured at Line Number 4, 15 days after the passage of the EPB shield.

The conventional empirical model [Eq. (1)] fits the measured surface settlement trough with measured centerline settlement,  $u_y^0 = 30.5$  mm, and fitted inflection width ratio,  $x_i/H = 0.42$  {hence, the apparent tunnel volume loss  $\Delta V_L/V_0 = \sqrt{2/\pi}[(x_i/R)(u_y^0/R)] = 3.1\%$ }.

The input parameters for the analytical solutions can be obtained by the three-point matching procedure proposed by Pinto (1999). The lateral displacement at the spring line can be interpreted from the inclinometer data,  $u_x^0 = 21.1$  mm. It is important to note that the N-2

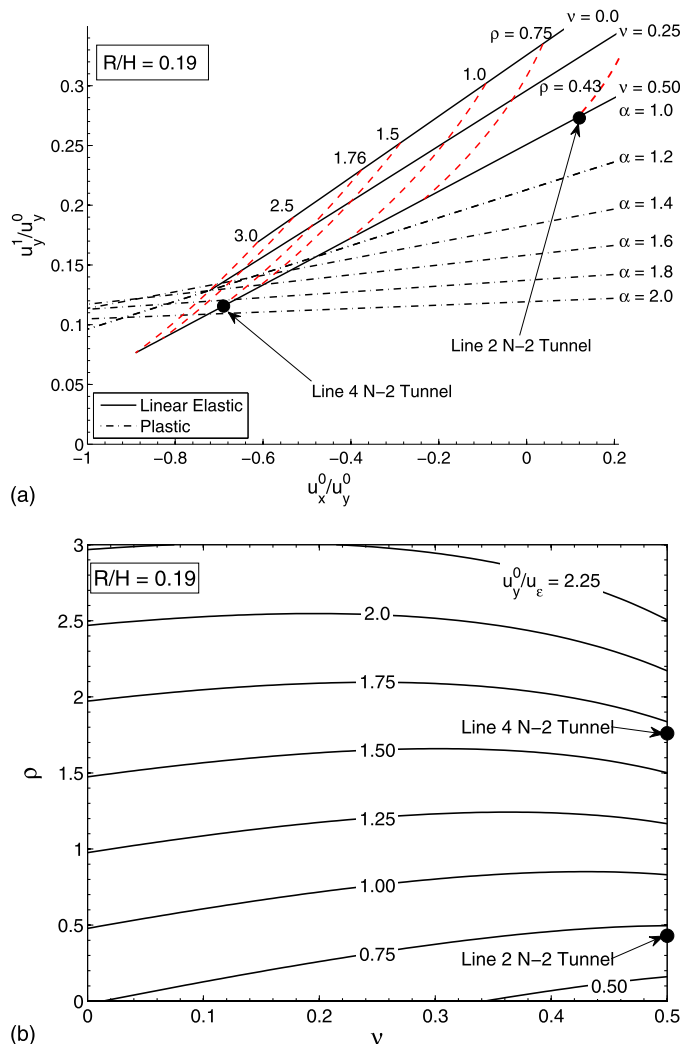


**Fig. 5.** Illustration of three-point measurement procedure for estimating input parameters: (a) determination of  $r$ ,  $\nu$ , or  $\alpha$ ; (b) determination of  $u_\epsilon$

tunnel caused outward movements of the ground at this location as a result of the high face pressure imposed during construction at this section and the low  $K_0$  conditions expected in the Recent Bay Mud. This result contradicts conventional empirical assumptions [cf. Eq. (3)]. The third parameter  $u_y^1$  was not measured directly, as there were no surface settlement measurements at offsets,  $|x/H| > 0.6$ . However, assuming that undrained conditions prevail and hence,  $\nu = 0.5$  (or  $\alpha = 1$ ), unique analytical solutions are obtained with measurement ratios  $u_x^0/u_y^0 = -0.69$  and  $u_y^1/u_y^0 = 0.12$ , as shown in Fig. 5(a) (hence,  $u_y^1 = 3.5$  mm) for a relative distortion,  $\rho = 1.76$ . Hence, the tunnel cavity parameters are derived as  $u_\epsilon = -17.9$  mm, with an equivalent volume loss,  $\Delta V_L/V_0 = 2.0\%$  [Fig. 5(b)].

Fig. 6(a) shows the more complete evaluation of the analytical input parameters at Line Number 4 using a least-squares fitting approach with a total of five surface settlement and 23 subsurface horizontal and vertical displacement component measurements (Clough et al. 1983). The results show significant differences between the LSS and constrained LSS\* solutions, mainly as a result of significant asymmetry observed in the field measurements. The measured asymmetry can be attributed in part to variations in stratigraphy that are not considered in the analytical solutions. Input parameters for the LSS\* solution,  $\rho = 2.11$  and



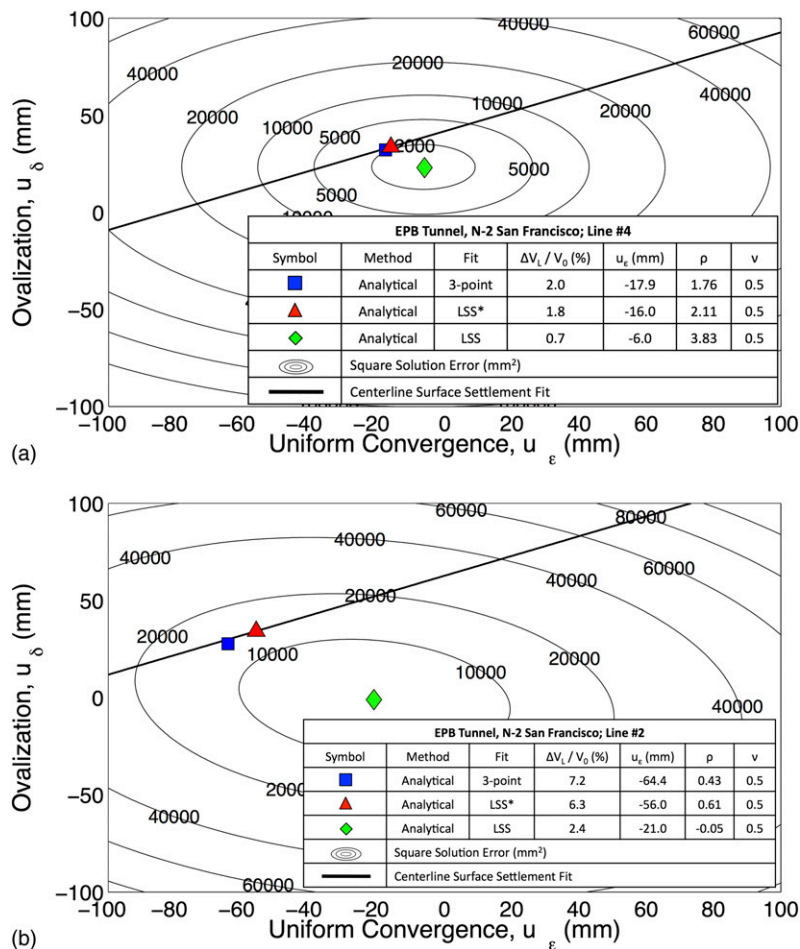


**Fig. 6.** Illustration of least-squares procedures for input parameter selection using N-2 case study, San Francisco: (a) N-2: Line Number 4; (b) N-2: Line Number 2

$u_\epsilon = -16$  mm (with an equivalent volume loss  $\Delta V_L / V_0 = 1.8\%$ ) differ only slightly from the simpler three-point matching procedure.

Figs. 7(a and b) compare the analytical (LSS\* and three-point) solutions with the measured vertical and lateral displacement components. The results show a very reasonable match to the distribution of ground movements around the tunnel, and provide a clear indication of the importance of the ovalization mode ( $u_\delta$ ) in explaining tunnel-induced ground movements and in estimating the volume loss associated with the tunneling process.

Similar methods of parameter selection have been applied to data from instrumentation Line Number 2 of the N-2 project, where a much lower face pressure was used ( $p/\gamma H = 0.4$ ). Fig. 8 shows that the two independent measurements ( $u_y^0 = 45.7$  mm,  $u_x^0 = -5.3$  mm, and  $u_x^0/u_y^0 = 0.12$ ) imply a much lower distortion ratio,  $\rho = 0.43$  at this section, and not surprisingly much higher ground loss than at Line Number 4 [ $u_\epsilon = -64.4$  mm and  $\Delta V_L / V_0 = 7.2\%$ ]; Fig. 6(b)]. The least-squares fitting analysis considered 20 subsurface displacement measurements and the centerline surface settlement  $u_y^0$  (the surface settlement trough was not surveyed at this section) as shown in Fig. 6(b). The LSS\* solution ( $\rho = 0.61$ ,  $u_\epsilon = -56$  mm, and hence  $\Delta V_L / V_0 = 6.3\%$ ) is again in reasonable agreement with the simpler three-point matching solution and both provide consistent estimates of the distribution of ground movements at Line Number 2 as shown in Fig. 8.

### Mexico City Sewer Tunnel

The tunnel considered in this section is part of the sewerage system of the Mexico City metropolitan area. The excavation was made with a shield and pressurized slurry at the tunnel face. Precast segmental linings were installed and at the same time grouting was used to fill the gap between the ring and tunnel wall (Romo 1997). Tunneling was undertaken through soft clay deposits, underlying approximately 6 m of silt and clay partings as shown in Fig. 9(b). The tunnel has a circular cross section of radius  $R = 2$  m and a depth to tunnel spring line  $H = 12.75$  m ( $R/H = 0.157$ ). Using the measured ground displacement ratios,  $u_x^0/u_y^0 = -0.41$  and  $u_y^1/u_y^0 = 0.23$ , Pinto (1999) obtained three-point matching parameters  $u_\epsilon = -22$  mm ( $\Delta V_L / V_0 = 2.2\%$ ),  $\rho = 1.53$ , and  $\nu = 0.12$ . While these parameters produce very reasonable agreement with the subsurface movements as shown in Fig. 9, the low value of  $\nu$  is difficult to justify. In fact, Romo (1997) reports a 1-m-thick sand seam at the elevation of the spring line. Pinto (1999) also found that the parameters are strongly affected by the accuracy of the measured value,  $u_x^0$  (and hence, the accuracy of a single reference inclinometer). The least-squares analysis uses 26 displacement components, including lateral displacements from three inclinometers and settlements at three elevations. The analysis also assumes undrained behavior of the soil (i.e.,  $\nu = 0.5$ ) to produce an LSS\* solution with input parameters  $u_\epsilon = -25$  mm ( $\Delta V_L / V_0 = 2.5\%$ ) and  $\rho = 1.34$ .

**Table 1.** Summary of Case Studies

Project	References	Construction method	Face conditions	$R$ (m)	$H$ (m)	Method	Input parameters			
							$\nu$ or [ $\alpha$ ]	$u_\epsilon$ (mm)	$\Delta V_L/V_0$ (%)	$\rho$
N-2 San Francisco: Line Number 4	Clough et al. (1983)	EPB	Soft clay	1.85	9.7	Three-point	0.5	-17.9	2.0	1.76
						LSS*	0.5	-16.0	1.8	2.11
N-2 San Francisco: Line Number 2						Three-point	0.5	-64.4	7.2	0.43
						LSS*	0.5	-56.0	6.3	0.61
Mexico City sewer	Romo (1997)	Slurry shield	Soft clay	2.00	12.8	Three-point	0.12	-22.0	2.2	1.53
						LSS*	0.5	-25.0	2.5	1.34
Madrid Metro extension: Line 1, Section 7	González (2002)	Open face (Belgian)	Very stiff clay	4.44 <sup>a</sup>	15.2	Three-point	0.5	-13.5	0.6	0.22
						LSS*	0.5	-14.0	0.6	0.21
						S&G	0.5	-17.0	0.8	0.20
Second Heineoord Heathrow Express trial tunnel (Type 3)	van Jaarsveld et al. (1999) Deane and Bassett (1995)	Slurry shield Open face NATM	Dense sand	4.15	16.7	LSS*	[1.09]	-26.0	1.3	0.80
			Very stiff clay	4.25 <sup>b</sup>	19.0	Three-point	0.5	-46.7	2.20	0.26
Milan Underground extension	Migliazza et al. (2009)	EPB shield	Sandy gravel	3.25	10.5	LSS*	[1.25]	-6.0	0.37	3.62
					11.5			-7.0	0.43	2.85
					13.5			-4.0	0.25	3.81

<sup>a</sup>Equivalent radius: horseshoe-shaped section.

<sup>b</sup>Equivalent radius: New Austrian Tunneling Method (NATM) section.

Fig. 9(a) compares the analytically computed and measured settlement troughs at three elevations ( $y = 0, -5, \text{ and } -10$  m) within the overlying clay layer. The model predictions are generally in good agreement with the field measurements except at locations close to the tunnel centerline, where both sets of analytical solutions overestimate the measured settlements. Fig. 9(b) compares the analytically computed and measured lateral displacements at three inclinometer positions ( $x = -2.5, 2.5, \text{ and } 4.5$  m). It is observed that the analytical solutions successfully capture the distribution of lateral movements caused by slurry-shield tunnel excavation. Surprisingly, the three-point matching provides better agreement with the measured data than the LSS\* solutions.

### Madrid Metro Extension

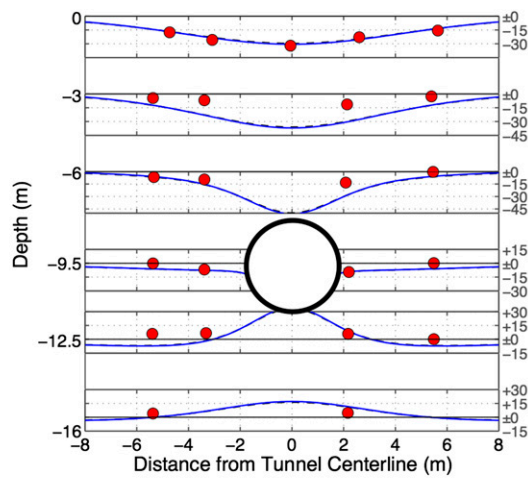
Approximately 20% of the extension of the Madrid Metro system (1995–1999) was constructed using the so-called Belgian Method, a special type of top heading and bench excavation (González and Sagasetta 2001) within tertiary deposits comprising stiff, overconsolidated clays covered by quaternary sediments. Fig. 10 summarizes the field measurements from a typical section (Line 1, Section 7; González 2002) that include surface settlements and lateral displacements recorded in a single inclinometer (at  $x = -8$  m). The tunnel has a horseshoe-shaped area of  $62 \text{ m}^2$  (equivalent circular radius,  $R_{eq} = 4.44$  m), a depth to spring line  $H = 15.2$  m, and an embedment ratio  $R/H = 0.29$ .

The input parameters suggested by the three-point matching technique correspond to  $u_\epsilon = -13.5$  mm ( $\Delta V_L/V_0 = 0.6\%$ ),  $\rho = 0.22$ , and  $\nu = 0.5$ , and are similar to values reported independently by González (2002). The LSS\* solution using all of the available field measurements produces  $u_\epsilon = -14$  mm ( $\Delta V_L/V_0 = 0.6\%$ ),  $\rho = 0.21$ , and  $\nu = 0.5$ , and all three solutions describe very well the measured ground movements. The small values of relative distortion may reflect details of the excavation sequence and the high  $K_0$ , strength and stability of the overconsolidated clay.

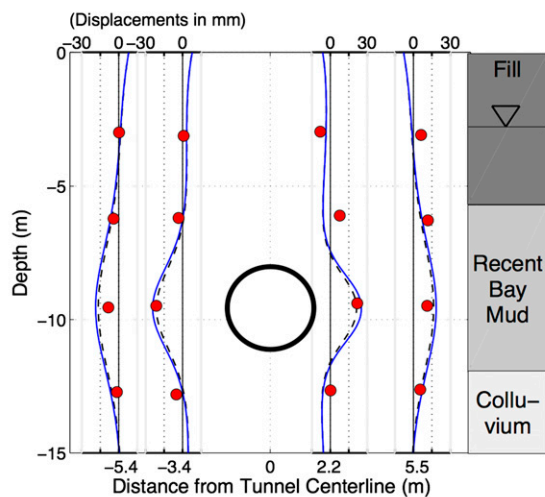
### Second Heineoord Tunnel

The second (tweede) Heineoord tunnel was built to relieve the large traffic volumes in the existing Heineoord tunnel, which crosses under the river Oude Maas, south of Rotterdam. The Dutch Ministry of Transportation selected the second Heineoord tunnel to be the pilot project for the construction of shield-driven tunnels in the Netherlands, because it was the first time that the shield-tunneling technique was used in the country (van Jaarsveld et al. 1999). The soil stratigraphy at the instrumented site comprises a 17-m-deep Holocene layer that mainly consists of loose to medium sands, overlying an 8-m-deep layer of dense to very dense sands, followed by 2 m of stiff silty clays and dense sands (Fig. 11). The average groundwater table was 3 m below ground level. Construction of the tunnel began in 1996 and was completed in June 1997. The tunnel consisted of twin tubes, each with a radius  $R = 4.15$  m and depth to spring line  $H = 16.65$  m ( $R/H = 0.25$ ). Tunnel-induced ground movements were extensively monitored with numerous surface settlement markers, six extensometers that measured subsurface settlements at six elevations and four inclinometers that measured horizontal displacements at the locations shown in Fig. 11.

Because the tunnel was constructed in sand, it is expected that volume changes will take place as a result of drained shearing within the soil mass and hence, the most appropriate framework, are the analytical solutions for a plastic, dilating soil. However, the measurement ratios  $u_x^0/u_y^0 = 0.07$  and  $u_y^1/u_y^0 = 0.04$  at this site fall outside the range of behavior expected from the three-point design charts [cf. Fig. 5(a) with  $R/H = 0.25$ ]. A least-squares solution was obtained using the displacement component data shown in Fig. 11 generating an LSS\* solution with  $u_\epsilon = -26$  mm ( $\Delta V_L/V_0 = 1.3\%$ ),  $\rho = 0.80$ , and  $\alpha = 1.09$ . These analyses describe very well the distribution of vertical displacements throughout the soil mass. The results for the lateral displacements are also in good agreement with the measured data except at locations within the inclinometer nearest to the tunnel and at two elevations close to the spring line. Fig. 11



(a) Vertical Displacements



(b) Lateral Displacements

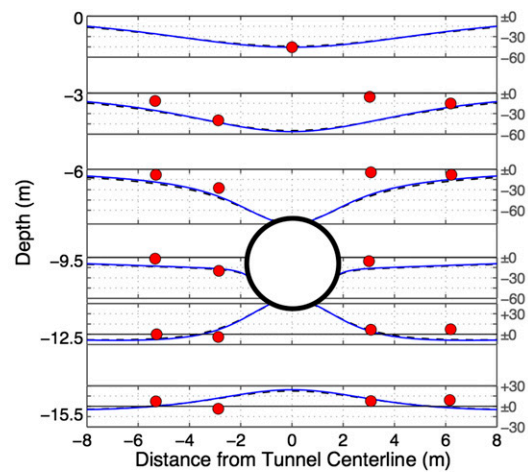
EPB Tunnel, N-2 San Francisco; Line 4						
Line	Method	Fit	$\Delta V_c / V_0$ (%)	$u_e$ (mm)	$\rho$	$\nu$
-----	Analytical	3-point	2.0	-17.9	1.76	0.5
—————	Analytical	LSS*	1.8	-16.0	2.11	0.5

**Fig. 7.** Computed and measured displacements for N-2 tunnel, San Francisco; Line 4: (a) vertical displacements; (b) lateral displacements

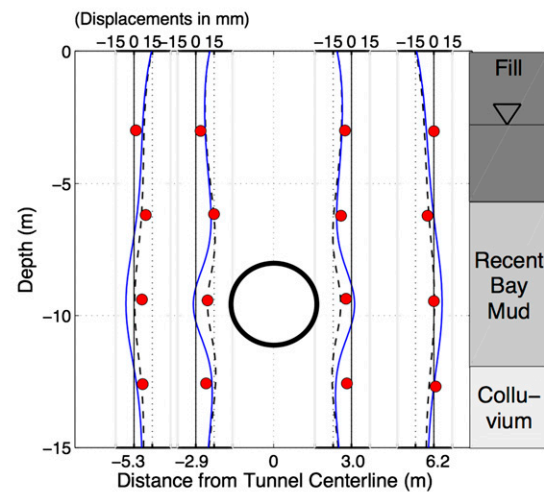
shows that when these two near-field points are excluded from the LSS analysis, the plastic (average dilation) solution gives remarkably good predictions of the ground deformation field for the second Heinenoord tunnel.

### Heathrow Express Trial Tunnel

The Heathrow Express (HEX) trial tunnel was built in 1992 to examine local ground response to three different sequential construction procedures in London clay, each over a length of 30 m (Deane and Bassett 1995). The current analyses focus on the Type 3 sequence, which comprised a top heading and bench sequence, with the bottom of the heading supported on inverted shotcrete arches to limit excess settlement. Ground movements are analyzed for the end of the construction phase (May 29, 1992). The local stratigraphy



(a) Vertical Displacements



(b) Lateral Displacements

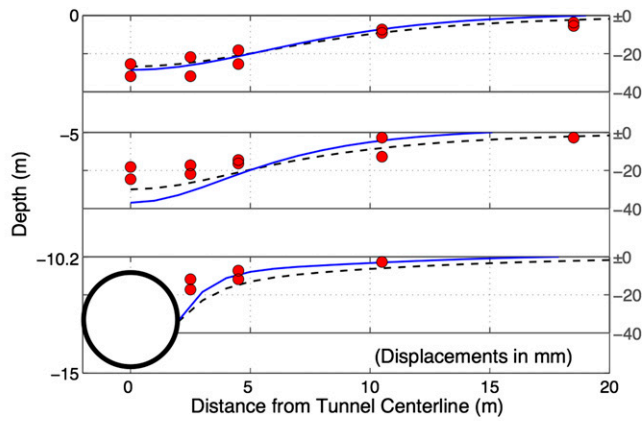
EPB Tunnel, N-2 San Francisco; Line 2						
Line	Method	Fit	$\Delta V_c / V_0$ (%)	$u_e$ (mm)	$\rho$	$\nu$
-----	Analytical	3-point	7.2	-64.4	0.43	0.5
—————	Analytical	LSS*	6.3	-56.0	0.61	0.5

**Fig. 8.** Computed and measured displacements N-2 tunnel, San Francisco; Line 2: (a) vertical displacements; (b) lateral displacements

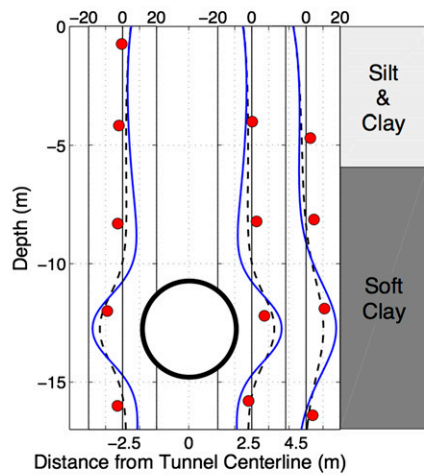
comprised 1–2 m of made ground and 2–4 m of dense terrace gravels overlying a deep layer of stiff, heavily overconsolidated London clay (more than 45 m thick). The trial tunnel was excavated entirely within the London clay, as shown in Fig. 12. The ground movements induced by the excavation of the tunnel were measured from a virtually greenfield site, with no significant structures in the zone of influence and the instrumentation used to measure the ground movements included leveling pins for surface movements and four inclinometers for subsurface horizontal movements. The key geometric parameters of the tunnel are depth to spring line,  $H = 19$  m, and equivalent circular radius,  $R = 4.25$  m ( $R/H = 0.22$ ).

The three-point parameter selection technique cannot be directly applied for this case as the measured ratios  $u_x^0/u_y^0 = 0.36$  and  $u_y^1/u_y^0 = 0.10$  are outside the bounds expected from the analytical solutions [cf. Fig. 5(a) with  $R/H = 0.22$ ]. Fig. 12 illustrates the dilemma for this case study. By assuming incompressibility of





(a) Vertical Displacements

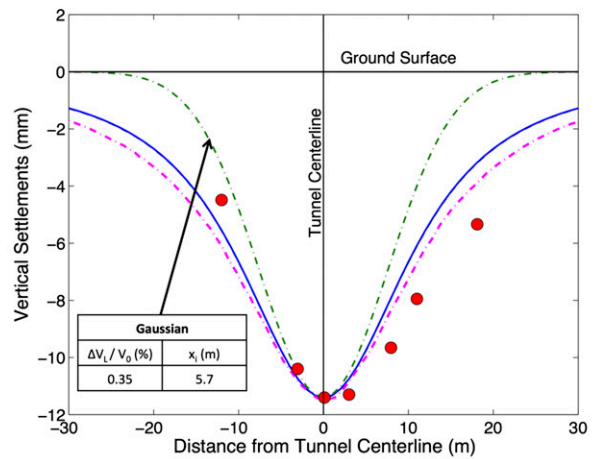


(b) Lateral Displacements

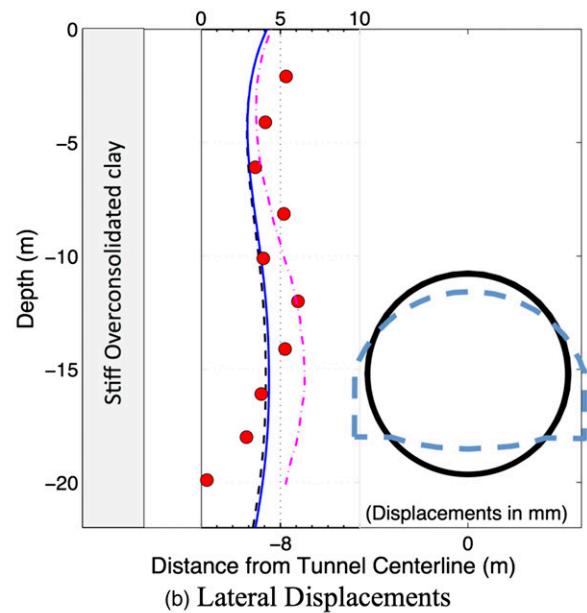
EPB Tunnel, Sewer tunnel Mexico City						
Line	Method	Fit	$\Delta V_t / V_0$ (%)	$u_e$ (mm)	$\rho$	$\nu$
-----	Analytical	3-point	2.2	-22	1.53	0.12
—————	Analytical	LSS*	2.5	-25	1.34	0.5

**Fig. 9.** Computed and measured displacements for EPB sewer tunnel, Mexico City: (a) vertical displacements; (b) lateral displacements

the soil ( $\nu = 0.5$ ) and matching two measurements ( $u_y^0$  and  $u_x^0$ ) the analytical solutions achieve excellent agreement with the distribution of horizontal displacements as shown in Fig. 12(b). However, the analyses predict a much wider settlement trough than is found in the measurements [Fig. 12(a)]. The least-squares approach uses all of the available displacement component data (excluding potentially misleading near-field points close to the tunnel cavity). The corresponding LSS\* solution achieves a modest improvement in the computed settlement trough shape [Fig. 12(a)] but matches only the shallow subsurface horizontal movements (for depths up to 10 m). Other researchers have attributed the narrow surface settlement trough of the HEX trial tunnel to effects of anisotropic stiffness and small strain nonlinearity of the high-overconsolidated London Clay (e.g., Simpson 1999; Stallebrass et al. 1994). Zymnis et al. (2013) also considered the effects of cross-anisotropic elastic properties on the analytical solutions using another open-face tunnel project in London.



(a) Surface Settlements



(b) Lateral Displacements

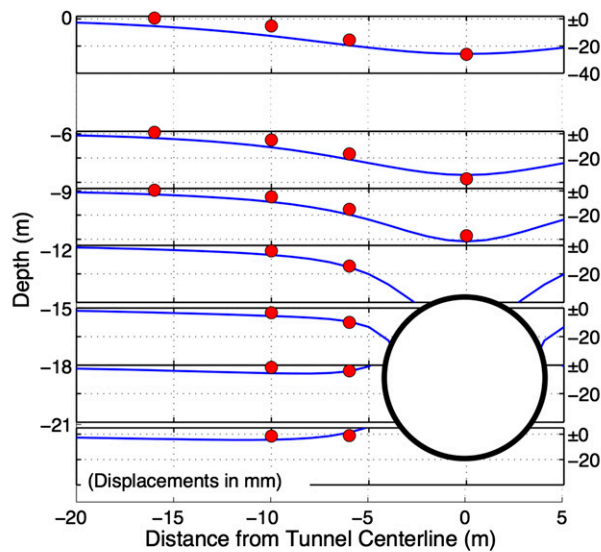
Open face tunnel, Madrid Metro Extension						
Line	Method	Fit	$\Delta V_t / V_0$ (%)	$u_e$ (mm)	$\rho$	$\nu$
-----	Analytical	3-point	0.6	-13.5	0.22	0.5
—————	Analytical	LSS* (17 points)	0.6	-14.0	0.21	0.5
- · - · - · -	Analytical (Gonzalez & Sagaseta, 1999)	3-point	0.8	-17.0	0.20	0.5

**Fig. 10.** Computed and measured displacements for Madrid Metro extension tunnel Line 1; Section 7: (a) surface settlements; (b) lateral displacements

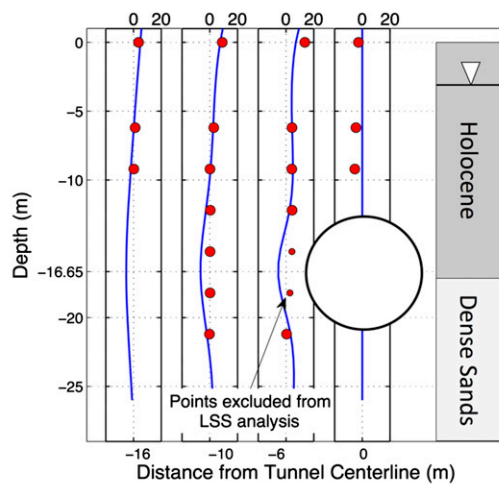
### Milan Underground Extension

The extension of Line 1 of the Metropolitana Milanese was constructed to connect the city of Milan to the new north metropolitan exhibition area and was completed in 2005 (Migliazza et al. 2009). The project involved construction of twin tunnels of total length of 2.1 km at depths varying from 8 to 19 m. The construction was carried out using an EPB Shield (EPB-S) machine with a cutter diameter of 6.54 m and prefabricated concrete lining rings with an outer diameter of 6.3 m. The clearance between the exterior of the lining and the soil mass was filled with grout injected at ports within





(a) Vertical Displacements



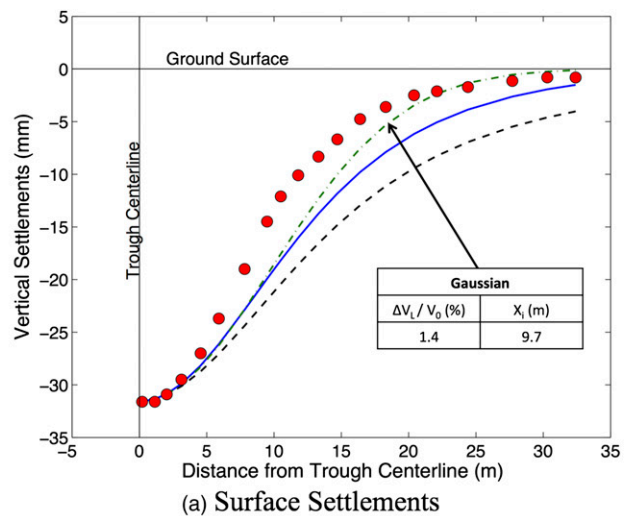
(b) Lateral Displacements

Shield driven slurry tunnel, Second Heine Noord Tunnel						
Line	Method	Fit	$\Delta V_L / V_0$ (%)	$u_\epsilon$ (mm)	$\rho$	$\alpha$
—	Analytical	LSS*	1.3	-26	0.82	1.095

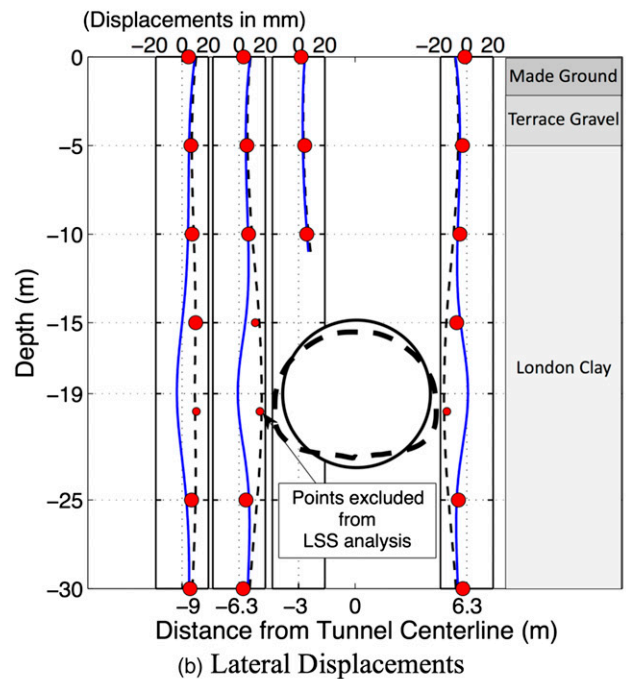
**Fig. 11.** Computed and measured displacements for second Heine Noord tunnel: (a) vertical displacements; (b) lateral displacements

the tail of the shield. All excavation took place in dense sandy gravels (relative density,  $D_r = 70\%$ ) of fluvioglacial and alluvial origin. Because the tunnels were excavated in sand, the soil paste in the working chamber was conditioned by means of foam and polymers.

Migliazza et al. (2009) present empirical, analytical, and numerical estimates of the surface settlements at three sections with different tunnel depths ranging from 10.5 to 13.5 m. Their interpretation of the analytical solutions (after González and Sagaseto 2001) was based on an assumed average dilatancy,  $\alpha = 1.21$  (corresponding to a maximum dilation angle,  $\psi = 10^\circ$  for the sands), while the cavity convergence,  $u_\epsilon$ , was found from the apparent volume loss (obtained from the measured settlement trough), and the ovalization,  $u_\delta$ , was based on results of independent numerical (finite-element) simulations.



(a) Surface Settlements



(b) Lateral Displacements

NATM Heathrow Express Trial Tunnel (Type 3)						
Line	Method	Fit	$\Delta V_L / V_0$ (%)	$u_\epsilon$ (mm)	$\rho$	$\nu$
- - - -	Analytical	3-point	2.2	-46.7	0.26	0.5
—	Analytical	LSS* (40 points)	1.5	-32.0	0.62	0.5

**Fig. 12.** Computed and measured displacements for New Austrian Tunneling Method (NATM) Heathrow Express trial tunnel: (a) surface settlements; (b) subsurface lateral displacements

In reassessing the same data, LSS\* optimizations were performed for this work (for  $u_\epsilon$  and  $u_\delta$ ) using the settlements measured at each of the three instrumented sections over a range of  $\alpha$  values. Fig. 13(a) shows that although there is no single optimal value of  $\alpha$  (based only on these limited surface settlement data),  $\alpha = 1.25$  produces identical least-squares error solutions for sections S5–28 and S5–29. For this selected value of  $\alpha$ , the optimized cavity parameters [Fig. 13(b)] generate very close agreement with the field measurements. The analyses show an average volume loss,  $\Delta V_L / V_0 = 0.35\%$  [slightly lower than the value interpreted by Migliazza et al. (2009)] and an

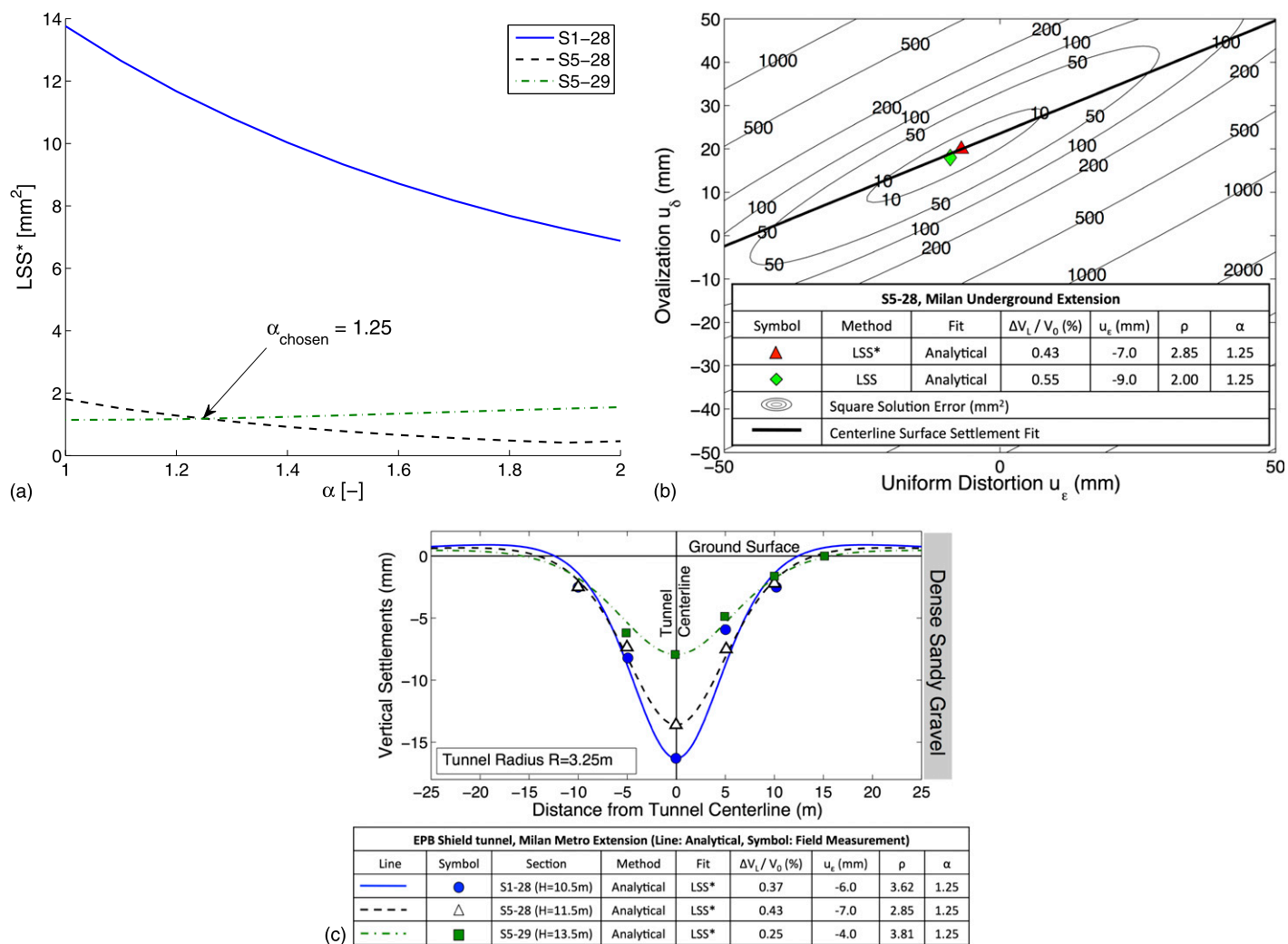


**Fig. 13.** Analysis of the Milan Underground extension project: (a) LSS\* versus  $\alpha$  for the three cross sections and selection of parameter  $\alpha$ ; (b) least-squares solution method for S5-28 and  $\alpha = 1.25$ ; (c) computed and measured surface settlements at three sections of the Milan Underground extension

average relative distortion  $\rho = 3.43$ . While this example highlights the practicality of the analytical solutions, their advantage relative to existing empirical solutions is only revealed when considering subsurface and lateral ground deformations.

## Conclusions

Analytical interpretations of far-field ground deformations (Pinto and Whittle 2013) have been compared with in situ measurements for construction of six tunnels excavated through different soils and using a variety of construction methods. This paper compares two different methods for selecting input parameters using (1) the three-point matching and (2) the least-squares fitting method. The three-point method relies on measurements of the surface centerline settlement  $u_y^0$ , trough width  $u_x^1$ , and lateral displacements at a reference spring line location  $u_x^0$ . When these are available and reliable, there is a very good matching with the least-squares solution. However, the least-squares technique appears less prone to error and has been used successfully on all of the reported case studies. The case studies presented in the paper include tunnels excavated by mechanical boring machines (EPB, slurry shield) and conventional tunneling in a variety of ground conditions. Volume losses

( $\Delta V_L / V_0 = -2u_e / R$ ) inferred from the data range from 0.25–7.2% with relative distortions  $\rho (= -u_\delta / u_e) = 0.20 - 3.81$ . Low volume loss and distortion parameters were obtained for open face excavation of the Madrid Metro extension project, in very stiff overconsolidated clay. The lowest volume loss was found for the Milan Underground extension which involved a modern EPB-shield excavation in dense sandy gravel. High volume losses for the N-2 tunnel in San Francisco were clearly linked to the control of face pressure in the soft clay conditions. Significant ovalization in this case also relates to the low  $K_0$  value of the Bay mud.

The analytical solutions describe very well the distributions of ground movements in five of the six cases presented, but appear to overestimate the width of the settlement trough for the construction of the Heathrow Express trial tunnel. This behavior may be attributed to anisotropic stiffness parameters that are considered elsewhere (Zymnis et al. 2013) or to nonlinear stiffness properties of the London clay. This work shows that the proposed analytical solutions represent a very attractive framework for estimating far-field ground displacements induced by tunnels when compared with purely empirical solutions while at the same time offer a very useful tool for checking more complex nonlinear numerical analyses.

## Acknowledgments

The original research (F. Pinto) on this topic was supported by a grant from the KKZ/CMA design-build team responsible for the Rio Piedras contract 7 of Tren Urbano in San Juan, Puerto Rico. The second author (D. M. Zymnis) also gratefully acknowledges support from the George and Maria Vergottis and Goldberg-Zoino fellowships for supporting her graduate studies at the Massachusetts Institute of Technology (MIT).

## References

- Attewell, P. B. (1978). "Ground movements caused by tunnelling in soil." *Proc., Int. Conf. on Large Movements and Structures*, J. D. Geddes, ed., Pentech Press, London, 812–948.
- Clough, G. W., Sweeney, B. P., and Finno, R. J. (1983). "Measured soil response to EPB shield tunneling." *J. Geotech. Engrg.*, 10.1061/(ASCE)0733-9410(1983)109:2(131), 131–149.
- Deane, A. P., and Bassett, R. H. (1995). "The Heathrow express trial tunnel." *Geotech. Eng.*, 113(3), 144–156.
- Finno, R. J., and Clough, G. W. (1985). "Evaluation of soil response to EPB shield tunneling." *J. Geotech. Engrg.*, 10.1061/(ASCE)0733-9410(1985)111:2(155), 155–173.
- González, C. (2002). "Deformaciones alrededor de túneles en suelos". Ph.D. thesis, Univ. de Cantabria, Cantabria, Spain.
- González, C., and Sagaseta, C. (2001). "Patterns of soil deformations around tunnels. Application to the extension of Madrid Metro." *Comput. Geotech.*, 28(6–7), 445–468.
- Kitiyodom, P., Matsumoto, T., and Kawaguchi, K. (2005). "A simplified analysis method for piled raft foundations subjected to ground movements induced by tunneling." *Int. J. Numer. Anal. Methods Geomech.*, 29(15), 1485–1507.
- Mair, R. J., and Taylor, R. N. (1997). "Bored tunneling in the urban environment." *Proc., 14th Int. Conf. on Soil Mechanics and Foundation Engineering*, Balkema, Rotterdam, Netherlands, 2353–2385.
- Migliazza, M., Chiorboli, M., and Giani, G. P. (2009). "Comparison of analytical method, 3D finite element model with experimental subsidence measurements resulting from the extension of the Milan underground." *Comput. Geotech.*, 36(1–2), 113–124.
- Möller, S. (2006). "Tunnel induced settlements and structural forces in linings." Ph.D. thesis, Institut für Geotechnik, Universität Stuttgart, Stuttgart, Germany.
- O'Reilly, M. P., and New, B. M. (1982). "Settlements above tunnels in United Kingdom—Their magnitude and prediction." *Proc., 3rd Int. Symp. Tunnelling 82*, Institute of Mining and Metallurgy, London, 173–181.
- Peck, R. B. (1969). "Deep excavations and tunnels in soft ground." *Proc., 7th Int. Conf. on Soil Mechanics and Foundation Engineering*, Sociedad Mexicana de Mecánica, Mexico, 225–290.
- Pinto, F. (1999). "Analytical methods to interpret ground deformations due to soft ground tunneling." S.M. thesis, Dept. of Civil and Environmental Engineering, Massachusetts Institute of Technology (MIT), Cambridge, MA.
- Pinto, F., and Whittle, A. J. (2013). "Ground movements due to shallow tunnels in soft ground. I: Analytical solutions." *J. Geotech. Geoenviron. Eng.*, 10.1061/(ASCE)GT.1943-5606.0000948, 04013040.
- Romo, M. P. (1997). "Soil movements induced by slurry shield tunneling." *Proc., 14th Int. Conf. on Soil Mechanics and Foundation Engineering*, Vol. 3, Balkema, Rotterdam, Netherlands, 1473–1481.
- Schmidt, B. (1969). "Settlements and ground movements associated with tunneling in soils." Ph.D. thesis, Univ. of Illinois, Urbana, IL.
- Simpson, B. (1999). "Engineering needs." *Proc., 2nd. International Symposium on Prefailure Deformation of Geomaterials*, Balkema, Rotterdam, Netherlands, 142–157.
- Stallebrass, S. E., Jovicic, V., and Taylor, R. N. (1994). "The influence of recent stress history on ground movements around tunnels." *Proc., Int. Symp. on Prefailure Deformation of Geomaterials*, Balkema, Rotterdam, Netherlands, 615–620.
- van Jaarsveld, E. P., Plekkenpol, J. W., and van de Graaf, C. A. M. (1999). "Ground deformations due to the boring of the second Heinenoord tunnel." *Proc., 12th European Conf. Geotechnical Engineering for Transportation Infrastructure*, F. B. J. Barends, J. Lindenberg, H. J. Luger, A. Verruijt, and L. de Quelerij, eds., Balkema, Rotterdam, Netherlands, 153–160.
- Vorster, T. E. B., Klar, A., Soga, K., and Mair, R. J. (2005). "Estimating the effects of tunneling on existing pipelines." *J. Geotech. Geoenviron. Eng.*, 10.1061/(ASCE)1090-0241(2005)131:11(1399), 1399–1410.
- Zymnis, D. M., Chatzigiannellis, Y., and Whittle, A. J. (2013). "Effect of anisotropy in ground movements caused by tunneling." *Géotechnique*, 63(13), 1083–1102.